Original Research Paper

Magnetization transfer saturation reveals subclinical optic nerve injury in pediatric-onset multiple sclerosis

Giulia Longoni, Edgar Martinez Chavez, Kimberly Young, Robert A Brown, Sonya Bells (iD), Dumitru Fetco (iD), Laura Kim, Stephanie A Grover, Fiona Costello (iD), Arun Reginald, Amit Bar-Or, Ruth Ann Marrie (iD), Douglas L Arnold (iD), Sridar Narayanan, Helen M Branson, Brenda L. Banwell, John G Sled, Donald J. Mabbott and E Ann Yeh (iD)

Abstract

Background: The presence of subclinical optic nerve (ON) injury in youth living with pediatric-onset MS has not been fully elucidated. Magnetization transfer saturation (MTsat) is an advanced magnetic resonance imaging (MRI) parameter sensitive to myelin density and microstructural integrity, which can be applied to the study of the ON.

Objective: The objective of this study was to investigate the presence of subclinical ON abnormalities in pediatric-onset MS by means of magnetization transfer saturation and evaluate their association with other structural and functional parameters of visual pathway integrity.

Methods: Eleven youth living with pediatric-onset MS (ylPOMS) and no previous history of optic neuritis and 18 controls underwent standardized brain MRI, optical coherence tomography (OCT), Magneto-encephalography (MEG)-Visual Evoked Potentials (VEPs), and visual battery. Data were analyzed with mixed effect models.

Results: While ON volume, OCT parameters, occipital MEG-VEPs outcomes, and visual function did not differ significantly between ylPOMS and controls, ylPOMS had lower MTsat in the supratentorial normal appearing white matter (-0.26 nU, $p = 0.0023$), and in both in the ON (-0.62 nU, $p < 0.001$) and in the normal appearing white matter of the optic radiation (-0.56 nU, $p = 0.00071$), with these being positively correlated ($+0.57$ nU, $p = 0.00037$).

Conclusions: Subclinical microstructural injury affects the ON of ylPOMS. This may appear as MTsat changes before being detectable by other currently available testing.

Keywords: Pediatric MS, magnetization transfer, optic nerve, optical coherence tomography, visual functions, quantitative MRI

Correspondence to:
G Longoni
Department of Neurosciences and Mental Health, The Hospital for Sick Children, 555 University Avenue, Toronto, ON M5G 1X8, Canada.
giulia.longoni@sickkids.ca

Giulia Longoni
E Ann Yeh
Division of Neurology, Department of Pediatrics, University of Toronto, Toronto, ON, Canada/ Department of Neurosciences and Mental Health, The Hospital for Sick Children, Toronto, ON, Canada

Edgar Martinez Chavez
Sonya Bells
Laura Kim
Donald J. Mabbott
Department of Neurosciences and Mental Health, The Hospital for Sick Children, Toronto, ON, Canada

Kimberly Young
Stephanie A Grover
Division of Neurology, Department of Pediatrics, University of Toronto, Toronto, ON, Canada

Robert A Brown
ShadowLab Research Inc., Toronto, ON, Canada

Dumitru Fetco
Sridar Narayanan
McConnell Brain Imaging Centre, Montreal Neurological Institute and Hospital, McGill University, Montreal, QC, Canada

Fiona Costello
Departments of Clinical Neurosciences and Surgery, Cumming School of Medicine, University of Calgary, Calgary, AB, Canada

Arun Reginald
Department of Ophthalmology and Visual Sciences, The University of Toronto, ON, Canada

Introduction

The optic nerve (ON) is often subclinically affected in MS. Subclinical optic nerve changes can be detected functionally,[1] and optical coherence tomography (OCT) has allowed precise and non-invasive quantification of subclinical retinal injury in patients with MS.[2–4] While conventional (clinically acquired) magnetic resonance imaging (MRI) has achieved fairly good sensitivity in detecting optic nerve signal changes during the acute phases of optic neuritis,[5–7] it is limited in its ability to detect more subtle changes in the asymptomatic patient. Quantitative MRI assessment of ON volume has consistently shown long-term tissue loss in the chronic phases after optic neuritis in adult patients with MS, with volume preservation in the non-affected eye.[8,9] Other quantitative MRI techniques like diffusion tensor imaging (DTI) of the optic nerve have also failed to demonstrate abnormalities in the non-affected MS eyes.[10] Magnetization transfer (MT) imaging is an MRI technique sensitive to myelin density and microstructural tissue integrity.[11,12] Others have used MT ratio (MTR) to investigate the degree and time course of optic nerve demyelination and microstructural alterations in patients with MS during and after optic neuritis, showing associations between the

degree of ON microstructural injury and the severity of visual outcomes.[2,13–17]

Recent years have seen the development of knowledge about the inter-relationships between subclinical, progressive retinal changes and brain microstructural alterations and atrophy, both reflecting aspects of common underlying mechanisms of disease progression.[18–20] However, studies assessing the clinically unaffected nerves of patients with MS with MTR have provided inconsistent results. Compared with healthy controls, some studies[2] showed lower MTR suggestive of subclinical ON abnormalities in asymptomatic people with MS, while others[15,16] showed no significant differences. These discrepancies could be due to the subtle nature of the changes but could also be due to inadequate sensitivity of the imaging technique. Due to the lengthy and technically complex image processing required to study the optic nerve with quantitative MRI, the analysis of in vivo ON microstructural changes, and whether these precede, follow, or mirror those seen in the retina and the retro-orbital brain, has lagged.[2,14,17] This has left a gap in knowledge regarding an important component in the characterization of structural changes that occur in MS at the level of the visual pathway. MT saturation (MTsat), a recently developed MT estimation method, may address this gap. MTsat compensates for T1 relaxation and flip angle inhomogeneities, thus overcoming important limitations of MTR imaging. MTsat is optimized to improve the contrast between white and gray matter and cerebrospinal fluid. Moreover, by improving the correlation with macromolecular content (e.g. myelin density), MTsat provides increased sensitivity to microstructural tissue changes and demyelination compared with MTR.[21]

We therefore sought to evaluate the ability of MTsat to show subclinical ON injury in a unique cohort of pediatric-onset MS patients with no previous known clinical optic neuritis event, and to explore the associations between these changes and those seen on structural and functional visual testing. Conceptually, a change in ON MTsat in such a cohort could derive from a combination of trans-synaptic degeneration from focal lesions within the optic radiations (OR) and/or chronic diffuse central nervous system demyelination and neurodegeneration involving the optic nerves as well as the whole brain. Therefore, with the hypothesis that an association between ON and retro-chiasmatic visual pathway integrity exists, we also studied the relationship between ON MTsat values and those in either the normal appearing white matter (NAWM) of the OR (OR$_{NAWM}$ MTsat), or *within* focal lesions along the OR (OR$_{lesions}$ MTsat).

Methods

Participants

Eleven youth living with pediatric-onset MS (ylPOMS) patients without a clinical history of optic neuritis were recruited at variable intervals from their initial presentation in the context of a prospective study of pediatric demyelination conducted in the Pediatric Neuroinflammatory Disorders Program at the Hospital for Sick Children (SickKids) between April 2017 and November 2018. Inclusion criteria were (1) a diagnosis of MS;[22] (2) age < 18 years at the time of enrollment; and (3) completion of standardized brain MRI, OCT, and visual battery that passed quality control.[23] Participants with a history of optic neuritis, MRI ON abnormalities on conventional imaging, or an interocular difference in retinal nerve fiber layer (RNFL) thickness greater than 5 μm[24] were excluded from the study. Participants with history of recent relapse (within 1 month of enrollment), MRI contraindications, comorbid psychiatric or neurological disorder, and Myelin oligodendrocyte glycoprotein (MOG) antibodies[25] were also excluded. Within 30 days of MRI acquisition, we also obtained demographic (sex, age) and basic neurologic data including disease history and neurological exam, as well as an extensive standardized functional visual assessment including OCT, MEG-visual evoked fields studies, perimetry, high-contrast visual acuity, color vision, and Low-contrast Visual Acuity (LCVA). Among the functional metrics collected, LCVA was chosen for our current analysis due to its excellent test–retest reliability and high sensitivity for visual dysfunction in MS.[26] In addition, we recruited 19 healthy pediatric participants as a control population.

MRI data acquisition and processing

All participants received standardized 3T MRI (MAGNETOM Prisma fit, Siemens Healthineers AG, Erlangen, Germany) including an axial T1-weighted MPRAGE (0.9 × 0.9 × 1.0 mm, TR: 1910 ms, TE: 3.51 ms, TI: 1100 ms, flip: 9°), sagittal fluid attenuated inversion recovery (FLAIR, 0.9 × 0.9 × 1.0 mm, TR: 6000 ms, TE: 356 ms, TI: 2200 ms), and a set of three scans comprising an MTsat acquisition (3D, 1.0 × 1.0 × 1.0 mm, TE: 3.82 ms; MToff: TR 33 ms, flip 10°; MTon: TR 33 ms, flip 10°, stock magnetization transfer preparation pulse; MTT1: TR 11 ms, flip 20°). B1 field mapping was also performed (2.0 × 2.0

Amit Bar-Or
Department of Neurology, Perelman School of Medicine, University of Pennsylvania, Philadelphia, PA, USA

Ruth Ann Marrie
Departments of Internal Medicine and Community Health Sciences, Max Rady College of Medicine, Rady Faculty of Health Sciences, University of Manitoba, Winnipeg, MB, Canada

Douglas L Arnold
McConnell Brain Imaging Centre, Montreal Neurological Institute and Hospital, McGill University, Montreal, QC, Canada/Department of Neurology and Neurosurgery, Montreal Neurological Institute and Hospital, McGill University, Montreal, QC, Canada

Helen M Branson
Department of Diagnostic Imaging, University of Toronto, Toronto, ON, Canada

Brenda L. Banwell
Division of Neurology, The Children's Hospital of Philadelphia, Perelman School of Medicine, University of Pennsylvania, Philadelphia, PA, USA

John G Sled
Department of Medical Biophysics, University of Toronto, Toronto, ON, Canada
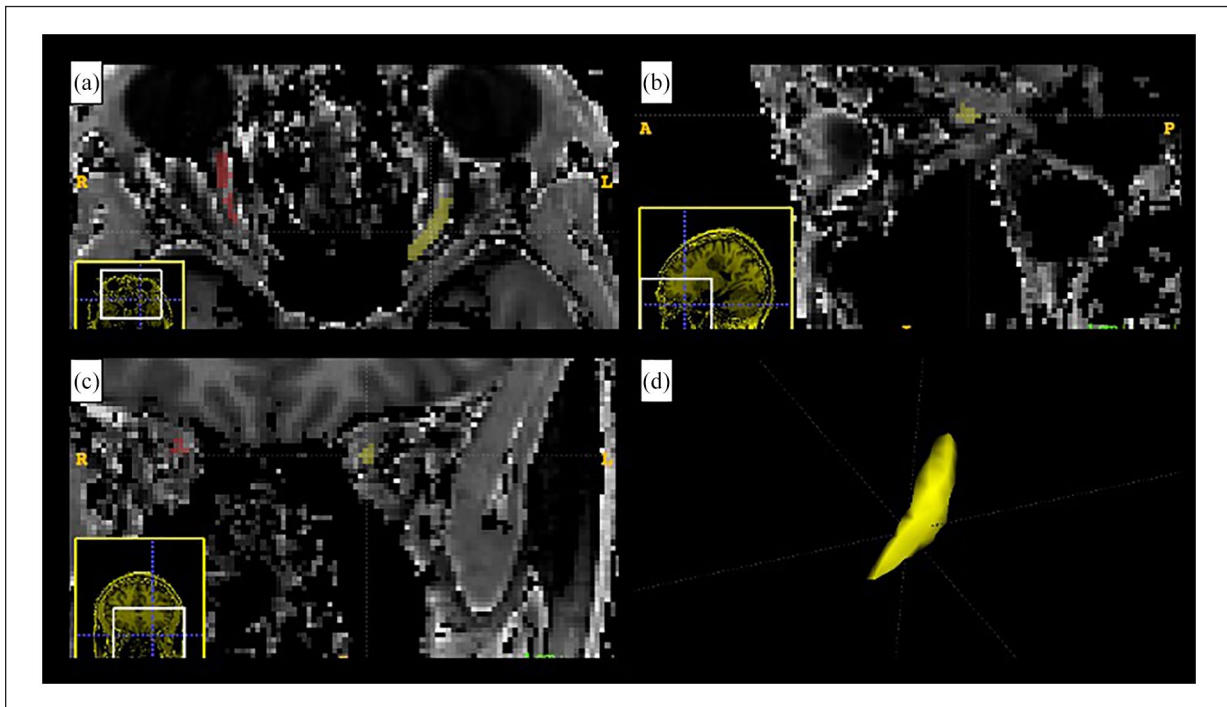
Figure 1. Example of segmentation. Axial (a), sagittal (b), and coronal (c) views from the manual segmentation of the optic nerves of a ylPOMS. The left optic nerve, shown in yellow, and the right optic nerve, in red, are visualized on the MTsat map of the subject. The panel in (d) shows, in yellow, the three-dimensional rendering of the segmented left intraorbital optic nerve (www.itksnap.org).

$\times$ 5.0 mm, TR 4000 ms, TE 18 ms, flip 60° and 120°). Brain tissue segmentation and supratentorial white matter (WM) lesion masks were obtained using a standardized pipeline as previously described.[27,28] The intraorbital ON segmentation for volume analysis was performed on T1-weighted MPRAGE images on multiplanar reformats by a single rater (KY) blinded to subjects' identity (www.itksnap.org). MTsat images were reconstructed as described in Helms, 2008,[21] and corrected for B_1 inhomogeneity. Co-registered MTon and MToff images and MTsat maps were carefully quality checked for the potential of movement artifact or misregistration between MTon, MToff, and MTsat images, and used to manually segment the left and right ON on MTsat maps by a single rater (GL) blinded to the subject's identity. Two healthy controls and one MS participant were excluded due to missing MTT1 sequence or failed quality control. To minimize movement and susceptibility artifacts, we included only voxels (1) contiguous to the geometrical center of the nerve; (2) that appeared to be part of the nerve on all three MT contrasts; and (3) within the posterior one-third of the intraorbital ON (Figure 1) (www.itksnap.org). To test intraobserver reproducibility of the intraorbital MPRAGE and MTsat segmentations, the scans of 10 randomly selected participants were evaluated twice at least 2 weeks apart; the intraclass correlation coefficient was 0.87 and 0.85, respectively. The John Hopkins University (JHU) DTI-based white matter atlas (ICGM-DTI-81)[29] was non-linearly registered to each participant's MTsat space to extract the bilateral OR using Advanced Normalization Tools (ANTS).[30] Supratentorial white matter (WM) lesion masks for each patient were subtracted from their supratentorial WM mask or their OR masks, and (1) average MTsat in the supratentorial NAWM (NAWM MTsat), (2) average MTsat along the ORs NAWM (OR_{NAWM} MTsat), and (3) average MTsat within OR WM lesions ($OR_{lesions}$ MTsat) were calculated and expressed in normalized MTsat Units (nU).

OCT data acquisition and processing. All scans were performed by trained personnel using a spectral domain OCT (SD-OCT) Cirrus scanner (Carl Zeiss Meditec 4000;7.0.3.19). Scanning was performed using the Optic Disc Cube 200×200 scan protocol for evaluation of the peripapillary RNFL, and the Macular Cube 512×128 scan protocol for that of ganglion cell-inner plexiform layer (GCIPL). Signal strength equal to or above 7 (out of 10) was considered adequate for analysis. RNFL and GCIPL were derived from data generated by the manufacturer's fully automated segmentation software. Peripapillary

RNFL was assessed by quadrants, and the average of all quadrants was reported as the mean RNFL thickness in micrometers (μm). GCIPL was measured in sextants and averaged to provide a mean GCIPL thickness (μm). Segmentation results were reviewed to ensure accuracy, with manual correction by trained OCT technicians where necessary.

VEPs data acquisition and processing. MEG data collection was conducted with a CTF whole-based 151 channel magnetoencephalography (MEG) system (VSM MedTech, Vancouver, Canada). The occipital MEG sensor peak response was used for the early visual evoked response according to the visual stimulus onset.

LCVA testing. All visual tests were administered monocularly. LCVA was assessed using a wall-mounted Pelli-Robson chart (Precision Vision, Woodstock, IL, USA) presented at 1 meter at eye level under standardized illumination conditions. LCVA was recorded as the lowest contrast sensitivity for which the participant correctly identified at least two of three triplet optotypes and reported as log units.

Statistical analysis. Statistical analysis was performed in Python 3.8.10 (python.org) using the NewModel module (https://github.com/robbbrown/NewModel, ShadowLab Research); model fitting was provided by lme4 1.1-27.1 in R-4.1.2 (r-project.org). Multivariable linear mixed effects models with unstructured matrix models were used to model ON MTsat, supratentorial NAWM MTsat, OR_{NAWM} MTsat, or ON volume in each *group* (ylPOMS, HC), accounting for *sex*, age, and a subject-specific random intercept accounting for correlations between left and right eye measurements of each participant. Except for *group* and *sex*, which were used as categorical variables, all the factors in the model were continuous variables. The association between ON MTsat and NAWM MTsat, OR_{NAWM} MTsat, $OR_{lesions}$ MTsat, ON volume, OCT parameters (RNFL thickness (RNFLT), temporal RNFLT ($RNFL_tT$), GCIPL thickness (GCIPLT)), MEG-VEPs outcomes (average occipital amplitude and latency) or LCVA was assessed within MS participants only with separate models including the same covariates. Chi-square tests comparing the log-likelihoods of the models with null models tested whether the model had significant explanatory power. Two R^2 values are provided for each model: the marginal R^2 is the proportion of the variance explained by the fixed effects only, and the conditional R^2 is the variance explained by the full

mixed model, including the random effects.[31] Normality of model residuals were checked to confirm goodness of fit and residuals were plotted to ensure homoscedasticity prior to using results. Results were not adjusted for multiple comparisons given the exploratory nature of this study.

Standard protocol approvals, registrations, and patient consents. Institutional Research Ethics Board approval (1000005356) and written informed consent (or assent and consent from a parent for younger children) from each participant and/or their guardian was obtained prior to study initiation.

Data availability. Qualified researchers may obtain access to all de-identified raw DICOM data and pre-processed images used for this study subject to appropriate ethical and legal considerations and in compliance with the appropriate Data Transfer/Sharing Agreement.

Results

The clinical and demographic characteristics of the two groups are reported in Table 1. Below, we report the results of the age- and sex-adjusted generalized mixed effect models. The full model fits are reported in the Appendix.

Differences between ylPOMS and HC
The predicted ON MTsat averaged 3.1 nU in HC (standard error (SE) = 0.47). ylPOMS showed lower ON MTsat than healthy participants (−0.62 nU, SE = 0.11; $p < 0.001$). Neither sex (males: −0.12 nU vs. females, SE = 0.11, $p = 0.26$) nor age (0.026 nU/year, SE = 0.0303, $p = 0.40$) affected mean ON MTsat (Figure 2). Average MTsat in the supratentorial NAWM and in the OR_{NAWM} were lower in ylPOMS compared with HC (−0.26 nU, SE = 0.075, $p = 0.0023$; and −0.56 nU, SE = 0.15, $p = 0.00071$, respectively). The predicted average ON volume was 68 mm³ (SE = 47). The model comparing ON volume between ylPOMS and HC was not significant (marginal $R^2 = 0.12$, conditional $R^2 = 0.89$, $p = 0.26$). None of the regression models assessing differences in RNFL (marginal $R^2 = 0.068$, conditional $R^2 = 0.92$, $p = 0.51$), temporal RNFL ($RNFL_t$) (marginal $R^2 = 0.072$, conditional $R^2 = 0.59$, $p = 0.40$), or GCIPL (marginal $R^2 = 0.16$, conditional $R^2 = 0.97$, $p = 0.14$) thickness, or MEG-VEPs outcomes (amplitude: marginal $R^2 = 0.15$, conditional $R^2 = 0.701$, $p = 0.15$; latency: marginal $R^2 = 0.081$, conditional $R^2 = 0.91$, $p = 0.49$) between ylPOMS and HC were significant.

Table 1. Demographics and clinical information of the study sample.

	ylPOMS (*n*=11)	HC (*n*=18)	Sig.[a]
Sex, F (%)	7 (64)	9 (50)	$\chi^2=0.51, p=0.47$
Age at onset (mean (range)) (years)	14.3 (11.7–17.4)	–	–
Age (mean (range)) (years)	16.7 (14.2–18.2)	15.6 (11–19.1)	$t=-1.7, p=0.108$
Disease duration (mean (range)) (years)	2.5 (0.15–6.2)	–	–
RNFL (mean[b] (range)) (µm)	91 (77–109)	96 (80–118)	$t=1.09, p=0.29$
RNFL$_{temporal}$ (mean[b] (range)) (µm)	62 (38–72)	67 (54–81)	$t=1.6, p=0.12$
GCIPL (mean[b] (range)) (µm)	80 (61–91)	84 (70–94)	$t=1.5, p=0.16$
ON MTsat (mean[b] (range)) (nU)	2.9 (2.5–3.2)	3.5 (2.9–4.2)	$t=5.9, p<10^{-5}$
ON volume (mean[b] (range)) (mm³)	96 (40–162)	87 (43–129)	$t=0.35, p=0.94$
NAWM MTsat (mean[b] (range)) (nU)	3.7 (3.2–4)	3.9 (3.7–4.1)	$t=3.4, p=0.002$
OR$_{NAWM}$ MTsat (mean[b] (range)) (nU)	3.5 (2.2–4.1)	4.1 (3.9–4.3)	$t=4.1, p=0.00031$
OR$_{lesions}$ MTsat (mean[b] (range)) (nU)	1.8 (0–2.7)	–	–
OR lesion volume (mm³)	387.1 (0–1735)	–	–
MEG-VEP p100 amplitude (mean[b] (range)) (µV)[c]	3.5 (2.8–4.9)	3.6 (2.1–6.0)	$t=-0.17, p=0.87$
MEG-VEP p100 latency (mean[b] (range)) (msec)[c]	120 (100–160)	110 (100–130)	$t=1.3, p=0.209$
LCVA (median (range)) (log units)[c]	1.58 (1.50–1.65)	1.65 (1.20–1.95)	$Z=0.52, p=0.603$

ylPOMS: youth living with pediatric-onset MS; RNFL: retinal nerve fiber layer; GCIPL: ganglion cell-inner plexiform layer; ON: optic nerve; MTsat: magnetization transfer saturation; NAWM: normal appearing white matter; OR: optic radiations; MEG: magnetoencephalography; HC: Healthy Controls; VEP: Visual Evoked Potential; LCVA: Low-contrast Visual Acuity.
[a]χ^2 test, two-tailed independent sample t-test, or two-tailed Mann–Whitney *U* test as appropriate.
[b]Left and right eye averaged.
[c]Five ylPOMS participants and one HC did not complete MEG-VEPs. One ylPOMS participant did not complete visual testing.

Relationship between ON MTsat and other structural visual pathway parameters (NAWM MTsat, OR$_{NAWM}$ MTsat, OR$_{lesions}$ MTsat), ON volume, OCT measures, MEG-VEPs outcomes, and LCVA in ylPOMS

In MS participants, lower ON MTsat was associated with lower OR$_{NAWM}$ MTsat (−0.57 nU for each one-unit decrease in ON MTsat, SE=0.14, *p*=0.00037). Lower ON MTsat was also associated with lower OR$_{lesions}$ MTsat (−0.048 nU for each one-unit decrease in ON MTsat, SE=0.23), although this was not statistically significant (*p*=0.84). ON MTsat was not significantly associated with supratentorial NAWM MTsat (−0.47 nU for each one-unit decrease in ON MTsat, SE=0.26, *p*=0.11). The regression models evaluating the association between ON volume, RNFLT, RNFL$_t$T or GCIPLT and ON MTsat were not significant (marginal R^2=0.13, conditional R^2=0.91, *p*=0.25; marginal R^2=0.041, conditional R^2=0.92, *p*=0.71; marginal R^2=0.12, conditional R^2=0.97, *p*=0.25; and marginal R^2=0.14, conditional R^2=0.79, *p*=0.46, respectively). Likewise, the three models assessing the relationship between average occipital MEG-VEP amplitude, latency, or LCVA, and ON MTsat did not reach statistical significance (amplitude: marginal R^2=0.16, conditional R^2=0.82, *p*=0.48; latency: marginal R^2=0.18, conditional R^2=0.77, *p*=0.47; LCVA:

marginal R^2=0.21, conditional R^2=0.87, *p*=0.29). However, we found an inverse relationship between ON volume and occipital MEG-VEP latency (+0.18 msec for each mm³ decrease in ON volume, SE=0.59 msec, *p*=0.045) in ylPOMS.

Discussion
In this study, we found lower ON MTsat and lower supratentorial NAWM and OR$_{NAWM}$ MTsat in ylPOMS compared with HC, and that higher MTsat in the ON correlated with higher MTsat in the OR$_{NAWM}$ in ylPOMS. Our results support the presence of early and diffuse microstructural changes affecting the anterior and posterior visual pathway in this population and suggest that ON subclinical injury may appear before being detectable by currently available structural and functional testing such as OCT and LCVA.[32,33]

The global decrease in MTsat parameters independent of previous episodes of optic neuritis, both in the supratentorial NAWM and in the visual pathway specifically, suggests that microstructural injury and demyelination might proceed in close conjunction in the ON and in the supratentorial WM, both being related to the diffuse and focal neurodegenerative aspects of MS pathobiology.
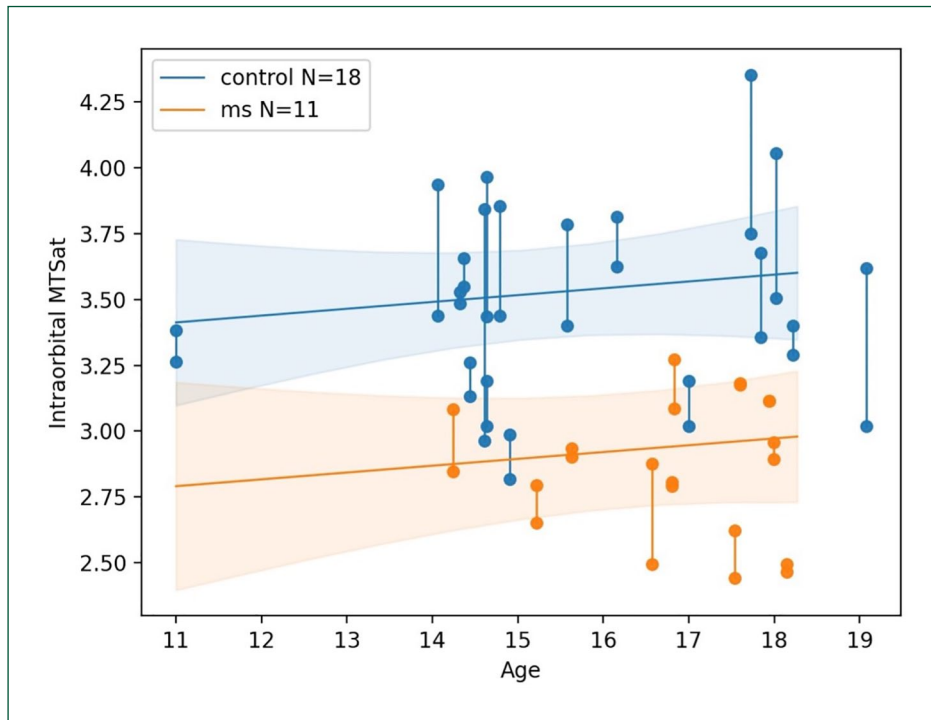
Figure 2. MTsat of the ON in ylPOMS and HC according to age.
The two lines of best fit represent the intraorbital ON MTsat values predicted by the model for each study group according to age. The points connected by vertical lines are values from the two eyes of individual participants. Shaded areas are 95% confidence intervals. Average intraorbital ON MTsat is expressed in normalized MT units [nU]. After accounting for sex (not shown) and age, ylPOMS show higher ON MTsat compared with HC.

We did not find statistically significant differences in retinal imaging parameters between our ylPOMS patients and the HC population. These results are generally in line with previous studies regarding OCT changes in non-affected eyes of ylPOMS patients[34,35] and confirm the relative preservation of retinal layer thicknesses in ylPOMS in the absence of previous ON episodes early in the MS disease course. Our results also suggest that MTsat may be more sensitive than OCT in detecting very early neurodegenerative processes in the visual pathway.

While others have found associations between ON MTR and OCT metrics in patients with MS and previous clinical evidence of optic neuritis,[2,14,17] our regression models investigating these associations with MTsat did not provide confident results and data fit. This is likely because of the small variation in the OCT parameters in our cohort of very early MS without previous episodes of optic neuritis, which did not differ significantly from those of HC.

As for the OCT parameters, the lack of a demonstrable relationship between ON MTsat and LCVA or MEG-VEPs outcomes was due to the lack of variation

in the visual and electrophysiological parameters, with absence of significant functional visual deficit in our study sample (all our MS participants had clinically normal vision).[36] A previous serial analysis of the ON following optic neuritis in adults with MS showed progressive decline of its cross-sectional area consistent with neuroaxonal loss over the span of 1 year, with no significant changes in the non-affected (fellow eye) compared with HC eyes.[8] Consistently, we did not find significant differences in ON volume between ylPOMS and HC. However, we found that lower ON volumes were associated with increased occipital MEG-VEP latencies in ylPOMS only. This may hint at a reduced structural and functional reserve in ylPOMS without previous episodes of optic neuritis, whereby even mild ON neuroaxonal loss can lead to loss of function reflected as increased evoked potential latencies.[8,35] Future studies involving MS participants with different degrees of impairment might contribute to a better understanding of the association between ON MTsat, ON volume, and visual functions.

Limitations of our technique involve possible misregistration of MTon-MToff during motion correction,

as well as the costs and the time associated with the image acquisition (approximately 30 minutes) and processing phase, and the ON manual segmentation (approximately 20–30 minutes per nerve). ON manual segmentation also makes the procedure intrinsically prone to bias due to the subjective nature of manual segmentation of anatomical structures. Limitations of our study include its small sample size and the cross-sectional nature of our data. Whether the detected changes in ON MTsat precede overt OCT and MEG-VEP abnormalities in ylPOMS is currently unknown. Future plans include the acquisition of prospective longitudinal data to follow the evolution of MTsat and visual pathway changes in early MS, as well as to determine the effect of optic neuritis on structural, functional, and electrophysiological visual outcomes in this population.

In conclusion, using MTsat we detected microstructural visual pathway and supratentorial NAWM alterations in pediatric-onset MS, even in the absence of abnormalities in visual function or structure using sensitive and well-established metrics. The changes we demonstrate might reflect subtle alteration of structure and maturation of neuroaxonal structure in the context of diffuse inflammation and demyelination, mirroring the results of other studies that have analyzed normal appearing brain tissues and volumes in pediatric onset MS.[27,37,38] Given the changes in MTsat we observed in the absence of abnormalities in OCT or LCVA, ON MTsat may be not only a research tool, but also potentially be translated clinically and of utility as an imaging metric for clinical trials focused on visual pathway outcomes in MS. Refinement of this technique with ON-dedicated sequences and automated processing would be required for use in clinical trials. Since the relative contributions of demyelination and axonal loss to reduction in MTsat cannot be established using this technique alone, future studies coupling other MRI techniques sensitive to injury to the axonal compartment, such as newer diffusion imaging techniques with computation of the axonal volume fraction, are needed.

ORCID iDs
Sonya Bells ⓘD https://orcid.org/0000-0001-8688-1571

Dumitru Fetco ⓘD https://orcid.org/0000-0003-1335-8274

Fiona Costello ⓘD https://orcid.org/0000-0001-8007-6627

Ruth Ann Marrie ⓘD https://orcid.org/0000-0002-1855-5595

Douglas L Arnold ⓘD https://orcid.org/0000-0003-4266-0106

E Ann Yeh ⓘD https://orcid.org/0000-0002-5393-7417

Supplemental material
Supplemental material for this article is available online.

References
1. Halliday AM, McDonald WI and Mushin J. Visual evoked response in diagnosis of multiple sclerosis. *Br Med J* 1973; 4: 661–664.

2. Trip SA, Schlottmann PG, Jones SJ, et al. Optic nerve magnetization transfer imaging and measures of axonal loss and demyelination in optic neuritis. *Mult Scler* 2007; 13(7): 875–879.

3. Henderson AP, Trip SA, Schlottmann PG, et al. An investigation of the retinal nerve fibre layer in progressive multiple sclerosis using optical coherence tomography. *Brain* 2008; 131(Pt. 1): 277–287.

4. Pulicken M, Gordon-Lipkin E, Balcer LJ, et al. Optical coherence tomography and disease subtype in multiple sclerosis. *Neurology* 2007; 69: 2085–2092.

5. Johnson G, Miller DH, MacManus D, et al. STIR sequences in NMR imaging of the optic nerve. *Neuroradiology* 1987; 29(3): 238–245.

6. Gass A, Moseley IF, Barker GJ, et al. Lesion discrimination in optic neuritis using high-resolution fat-suppressed fast spin-echo MRI. *Neuroradiology* 1996; 38(4): 317–321.

7. Chow LS and Paley MNJ. Recent advances on optic nerve magnetic resonance imaging and post-processing. *Magn Reson Imaging* 2021; 79: 76–84.

8. Hickman SJ, Toosy AT, Jones SJ, et al. A serial MRI study following optic nerve mean area in acute optic neuritis. *Brain* 2004; 127(Pt. 11): 2498–2505.

9. Harrigan RL, Smith AK, Lyttle B, et al. Quantitative characterization of optic nerve atrophy in patients with multiple sclerosis. *Mult Scler J Exp Transl Clin* 2017; 3(3): 2055217317730097.

10. Hickman SJ, Wheeler-Kingshott CA, Jones SJ, et al. Optic nerve diffusion measurement from diffusion-weighted imaging in optic neuritis. *AJNR Am J Neuroradiol* 2005; 26(4): 951–956.

11. Gareau PJ, Rutt BK, Karlik SJ, et al. Magnetization transfer and multicomponent T2 relaxation measurements with histopathologic correlation in an experimental model of MS. *J Magn Reson Imaging* 2000; 11(6): 586–595.

12. Schmierer K, Wheeler-Kingshott CA, Tozer DJ, et al. Quantitative magnetic resonance of postmortem multiple sclerosis brain before and after fixation. *Magn Reson Med* 2008; 59(2): 268–277.

13. Hickman SJ, Toosy AT, Jones SJ, et al. Serial magnetization transfer imaging in acute optic neuritis. *Brain* 2004; 127(Pt. 3): 692–700.

14. Frohman EM, Dwyer MG, Frohman T, et al. Relationship of optic nerve and brain conventional and non-conventional MRI measures and retinal nerve fiber layer thickness, as assessed by OCT and GDx: A pilot study. *J Neurol Sci* 2009; 282: 96–105.

15. Inglese M, Ghezzi A, Bianchi S, et al. Irreversible disability and tissue loss in multiple sclerosis: A conventional and magnetization transfer magnetic resonance imaging study of the optic nerves. *Arch Neurol* 2002; 59(2): 250–255.

16. Thorpe JW, Barker GJ, Jones SJ, et al. Magnetisation transfer ratios and transverse magnetisation decay curves in optic neuritis: Correlation with clinical findings and electrophysiology. *J Neurol Neurosurg Psychiatry* 1995; 59(5): 487–492.

17. Wang Y, van der Walt A, Paine M, et al. Optic nerve magnetisation transfer ratio after acute optic neuritis predicts axonal and visual outcomes. *PLoS ONE* 2012; 7(12): e52291.

18. Ngamsombat C, Tian Q, Fan Q, et al. Axonal damage in the optic radiation assessed by white matter tract integrity metrics is associated with retinal thinning in multiple sclerosis. *Neuroimage Clin* 2020; 27: 102293.

19. Puthenparampil M, Federle L, Poggiali D, et al. Trans-synaptic degeneration in the optic pathway. A study in clinically isolated syndrome and early relapsing-remitting multiple sclerosis with or without optic neuritis. *PLoS ONE* 2017; 12: e0183957.

20. Saidha S, Al-Louzi O, Ratchford JN, et al. Optical coherence tomography reflects brain atrophy in multiple sclerosis: A four-year study. *Ann Neurol* 2015; 78(5): 801–813.

21. Helms G, Dathe H, Kallenberg K, et al. High-resolution maps of magnetization transfer with inherent correction for RF inhomogeneity and T1 relaxation obtained from 3D FLASH MRI. *Magn Reson Med* 2008; 60(6): 1396–1407.

22. Thompson AJ, Banwell BL, Barkhof F, et al. Diagnosis of multiple sclerosis: 2017 revisions of the McDonald criteria. *Lancet Neurol* 2018; 17: 162–173.

23. Tewarie P, Balk L, Costello F, et al. The OSCAR-IB consensus criteria for retinal OCT quality assessment. *PLoS ONE* 2012; 7(4): e34823.

24. Waldman AT, Benson L, Sollee JR, et al. Interocular difference in retinal nerve fiber layer thickness predicts optic neuritis in pediatric-onset multiple sclerosis. *J Neuroophthalmol* 2020; 41: 469–475.

25. Kitley J, Waters P, Woodhall M, et al. Neuromyelitis optica spectrum disorders with aquaporin-4 and myelin-oligodendrocyte glycoprotein antibodies: A comparative study. *JAMA Neurol* 2014; 71(3): 276–283.

26. Balcer LJ, Raynowska J, Nolan R, et al. Validity of low-contrast letter acuity as a visual performance outcome measure for multiple sclerosis. *Mult Scler* 2017; 23(5): 734–747.

27. Longoni G, Brown RA, MomayyezSiahkal P, et al. White matter changes in paediatric multiple sclerosis and monophasic demyelinating disorders. *Brain* 2017; 140: 1300–1315.

28. Francis SJ. *Automatic lesion identification in MRI of multiple sclerosis patients*. MSc Thesis, Mcgill University, Montreal, QC, Canada, 2004.

29. Wakana S, Jiang H, Nagae-Poetscher LM, et al. Fiber tract-based atlas of human white matter anatomy. *Radiology* 2004; 230(1): 77–87.

30. Avants BB, Epstein CL, Grossman M, et al. Symmetric diffeomorphic image registration with cross-correlation: Evaluating automated labeling of elderly and neurodegenerative brain. *Med Image Anal* 2008; 12(1): 26–41.

31. Nakagawa S and Schielzeth H. A general and simple method for obtaining R2 from generalized linear mixed-effects models. *Methods Ecol Evol* 2013; 4: 133–142.

32. Pohl D, Rostasy K, Treiber-Held S, et al. Pediatric multiple sclerosis: Detection of clinically silent lesions by multimodal evoked potentials. *J Pediatr* 2006; 149(1): 125–127.

33. Yeh EA, Weinstock-Guttman B, Lincoff N, et al. Retinal nerve fiber thickness in inflammatory demyelinating diseases of childhood onset. *Mult Scler* 2009; 15(7): 802–810.

34. Graves JS, Chohan H, Cedars B, et al. Sex differences and subclinical retinal injury in pediatric-onset MS. *Mult Scler* 2016; 23: 447–455.

35. Waldman AT, Liu GT, Lavery AM, et al. Optical coherence tomography and visual evoked potentials in pediatric MS. *Neurol Neuroimmunol Neuroinflamm* 2017; 4(4): e356.

36. Sharma R, Joshi S, Singh KD, et al. Visual evoked potentials: Normative values and gender differences. *J Clin Diagn Res* 2015; 9(7): CC12–CC15.

37. Aubert-Broche B, Fonov V, Narayanan S, et al. Onset of multiple sclerosis before adulthood leads to failure of age-expected brain growth. *Neurology* 2014; 83: 2140–2146.

38. Rocca MA, Absinta M, Moiola L, et al. Functional and structural connectivity of the motor network in pediatric and adult-onset relapsing-remitting multiple sclerosis. *Radiology* 2010; 254(2): 541–550.